

Observed Statistical Behavior of Radar Moon Echo Signals

LORENZO J. ABELLA

*Space Technology Branch
Space Systems Division*

May 2, 1974



NAVAL RESEARCH LABORATORY
Washington, D.C.

SECURITY CLASSIFICATION OF THIS PAGE (When Data Entered)

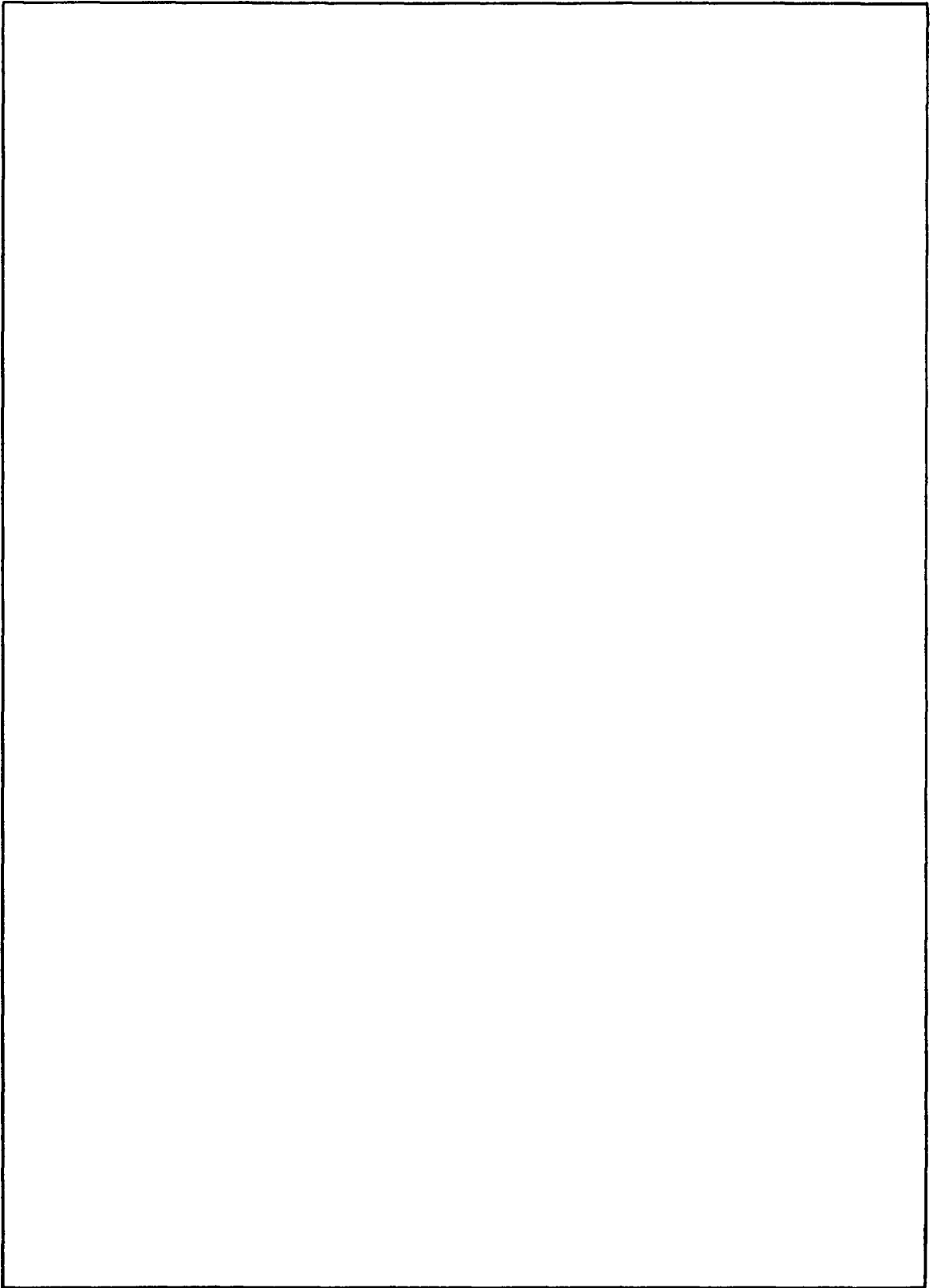
REPORT DOCUMENTATION PAGE		READ INSTRUCTIONS BEFORE COMPLETING FORM
1. REPORT NUMBER NRL Report 7717	2. GOVT ACCESSION NO.	3. RECIPIENT'S CATALOG NUMBER
4. TITLE (and Subtitle) OBSERVED STATISTICAL BEHAVIOR OF RADAR MOON ECHO SIGNALS		5. TYPE OF REPORT & PERIOD COVERED Interim Report
		6. PERFORMING ORG. REPORT NUMBER
7. AUTHOR(s) Lorenzo J. Abella		8. CONTRACT OR GRANT NUMBER(s)
9. PERFORMING ORGANIZATION NAME AND ADDRESS Naval Research Laboratory Washington, D. C. 20375		10. PROGRAM ELEMENT, PROJECT, TASK AREA & WORK UNIT NUMBERS NRL Problem R06-30 NAVELEX 63715N
11. CONTROLLING OFFICE NAME AND ADDRESS Department of the Navy Naval Electronic Systems Command Washington, D. C. 20360		12. REPORT DATE May 2, 1974
		13. NUMBER OF PAGES 21
14. MONITORING AGENCY NAME & ADDRESS (if different from Controlling Office)		15. SECURITY CLASS. (of this report) Unclassified
		15a. DECLASSIFICATION/DOWNGRADING SCHEDULE
16. DISTRIBUTION STATEMENT (of this Report) Approved for public release; distribution unlimited.		
17. DISTRIBUTION STATEMENT (of the abstract entered in Block 20, if different from Report)		
18. SUPPLEMENTARY NOTES		
19. KEY WORDS (Continue on reverse side if necessary and identify by block number) Statistical analysis Average waveform Ensemble autocorrelation Sample probability density functions Radar Moon echo signals		
20. ABSTRACT (Continue on reverse side if necessary and identify by block number) The observed statistical behavior of radar Moon echo signals at a transmitted radio frequency of 138.6 MHz has been analyzed. The results of the data analysis are in terms of plots for averaged Moon echoes, ensemble autocorrelation functions, and sample probability density functions at a fixed range. An empirical modeling of the data was attempted by curve fitting the results.		

DD FORM 1 JAN 73 1473

EDITION OF 1 NOV 65 IS OBSOLETE
S/N 0102-014-6601

i

SECURITY CLASSIFICATION OF THIS PAGE (When Data Entered)



CONTENTS

INTRODUCTION	1
PHYSICAL MECHANISM OF WAVE SCATTER	1
RADAR DATA	3
STATISTICAL CHARACTERISTICS	4
CONCLUDING REMARKS	16
ACKNOWLEDGMENT	16
REFERENCES	17

OBSERVED STATISTICAL BEHAVIOR OF RADAR MOON ECHO SIGNALS

INTRODUCTION

It is well known that radiation scattered from moving rough surfaces is random [1]. An example of a moving rough object encountered in radar astronomy is the Moon. The irregularity of the Moon's surface produces wave multiplicity, whereas lunar librations make this wave multiplicity variable in time, variable in a random way. Thus statistical properties of Moon echo data, such as average scattered power and fading rates, have been used in the past [2-10] to discuss theoretical rough surface models of the lunar terrain and Moon echo signal-processing techniques. It is the intent of this report to enlarge the statistical data base presently available in the literature on radar Moon echoes by presenting some results of a Moon bounce radar experiment conducted at the Naval Research Laboratory (NRL) on May 1, 1972.

In this report we shall be concerned with a statistical data analysis of the quasi-specular portion [9,10] of Moon echoes. The physical mechanisms for signal randomness are reviewed briefly. Relevant radar parameters used in this experiment and the data reduction scheme followed for processing in a digital computer are then discussed. Plots of averaged Moon echoes, ensemble autocorrelation functions, and Moon echo sample probability density functions at a fixed range are presented.

PHYSICAL MECHANISM OF WAVE SCATTER

As mentioned earlier, lunar librations constitute the physical mechanism behind random electromagnetic wave scatter from the lunar surface. The phenomenon of libration can be regarded as a slow rocking of the lunar disk as seen from the Earth. Because the Earth-Moon orbital lock is not perfect, small departures from synchronism take place, and the subterrestrial point approximately traces out an ellipse on the lunar surface over a one-month period in the selenographic quadrant $\pm 8^\circ$ latitude and $\pm 8^\circ$ longitude [3,5,9,10]. These are the so-called physical librations in latitude and longitude. In addition, there is a diurnal libration caused by the parallactic shift between the center of the Moon's disk and the true center of the Moon as the Earth rotates. This diurnal libration causes the subradar point to wander on the lunar surface by an additional 2° in latitude and longitude on any given day of the month. The total rate of libration ℓ_T seen by an Earth observer can be expressed as the projection normal to the line of sight of the vector sum of the physical and diurnal librations. An expression for ℓ_T is given by [5,10]

$$\ell_T = [(\ell_L + (12 \times 10^{-7}) \cos \phi \cos \delta \cos LHA)^2 + (\ell_\beta + (12 \times 10^{-7}) \cos \phi \sin \delta \sin LHA)^2]^{1/2}, \quad (1)$$

where

- ℓ_T = total rate of libration, in rad/s
 ϕ = site latitude
 LHA = local hour angle
 δ = maximum lunar declination during month
 ℓ_L = libration in longitude
 ℓ_β = libration in latitude.

The values of ℓ_L , ℓ_β , and δ may be obtained from tables of ephemeris for physical observations of the Moon listed in the *American Ephemeris and Nautical Almanac*. The LHA may be obtained from knowledge of Moon tracks at the site latitude. Figure 1 shows a plot of the total rate of libration ℓ_T (Eq. (1)) vs time for May 1, 1972 in the interval from moonrise to moonset, corresponding to the following parameters:

- ϕ = 38.52°
 δ = 7.79°
 ℓ_L = $-1.18^\circ/\text{day} = -2.37 \times 10^{-7}$ rad/s
 ℓ_β = $-0.96^\circ/\text{day} = -1.93 \times 10^{-7}$ rad/s

It is to be noted that the total libration rate reaches a broad maximum practically at meridian transit and drops by more than 75% at moonset. These are important features, as explained next.

Because of the Moon's librations, the lunar aspect at the subradar point changes with time. Since at UHF through SHF wavelengths the Moon can be considered to be a rough target [9], at these wavelengths there will be a randomly varying distribution of scattering centers with time, and the direction of the total reflected wave will change randomly in time. The projection of the scattered propagation vector along the specular line of sight will have, then, randomly varying intensities or fadings. If the lunar aspect changes very fast, i.e., a high libration rate exists, there will be rapid fades in the scattered radiation and the pulse-to-pulse correlation will be low. On the other hand for a small libration rate the returns, although diffuse, will be highly correlated. Typical values of the pulse-to-pulse correlation coefficient of echoes 1s apart have been shown to be [5] about 0.4 for periods of high fading rates and 0.98 for periods of low fading rates. Thus the *magnitude* of the libration rate plays a decisive role in determining the degree of randomness of the signal. Furthermore the *time rate of change* of the libration rate determines the extent of the stationarity of the random signal. It can be assumed that when the total change of the libration rate over some time interval is an arbitrarily small percent of the maximum libration rate, the resultant statistical properties over that time interval will be weakly stationary. Otherwise, the statistics can be assumed nonstationary. It is clear, then, that any determination of the random properties of the reflected radiation has to

take into consideration the time interval of the scattering, i.e., where on the libration curve the statistics were obtained. In Fig. 1 we show the time interval corresponding to the duration of the radar experiment reported on in this report. The timing was such that it encompassed the broad maximum of the libration rate, which provided for observations of radar moon echoes containing a high degree of signal randomness. Fig. 2 shows the time interval enlarged. We note that during the course of the experiment the libration rate ℓ_T fell by less than 10% of its maximum value; during the first 33 min. it changed by only 0.5%. We have assumed weak stationarity if the libration rate for a given time subinterval changed by less than 0.5%. Thus, the statistics presented in this report have been obtained over time subintervals that provided for weak stationarity within the stated limitations.

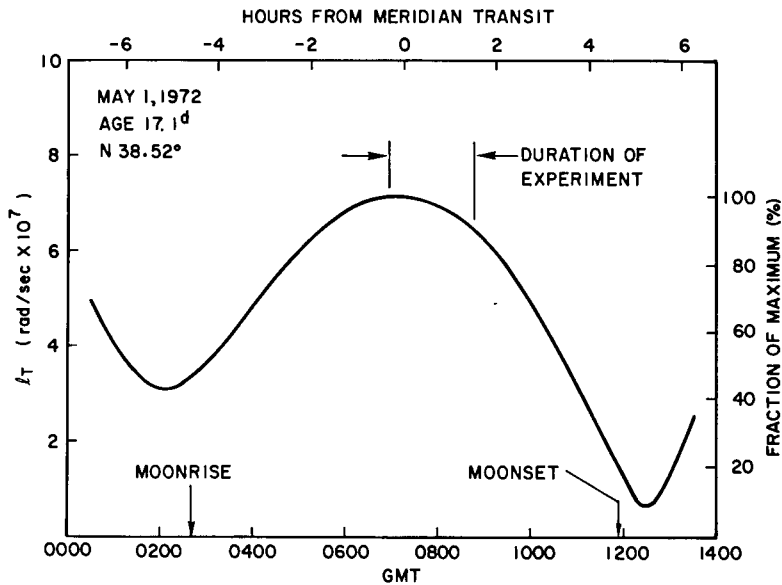


Fig. 1 — Total libration rate ℓ_T calculated from Eq. (1) for moonrise to moonset

RADAR DATA

The experiment took place on May 1, 1972 between 06^h56^m45^s and 08^h42^m03^s GMT. Electromagnetic pulses were transmitted from the 150-ft dish at NRL's Chesapeake Bay Division, Maryland, at a radio frequency of 138.6 MHz with circular polarization. These pulses had lengths of 10, 20, 50, 100 and 200 μ s and were beamed at the Moon continuously at pulse repetition frequencies (PRF) of 500, 250, 100, 50 and 25 Hz, respectively, by tracking the Moon as it swept across the sky. Acquisition of Moon echoes was effected at NRL's 150-ft dish in Sugar Grove, West Virginia, using similar tracking techniques. The reflected RF signals were frequency converted and recorded on magnetic tape at 120 inches per second (ips) as predetected 450-kHz IF pulses. The reduction of the data to a digital format was accomplished at NRL's Research Computation Center (RCC). Selected portions of the run were played back at 30 ips through a 100 kHz diode (envelope) detector and digitized in an 8-bit analog-to-digital (A/D) converter clocked at a 562.5-kHz sampling rate. A CDC 1604B digital computer received the output of

the digitizer, formatted the data, and recorded it on digital magnetic tapes. These tapes were later taken to a CDC-3800 computer for statistical data analysis.

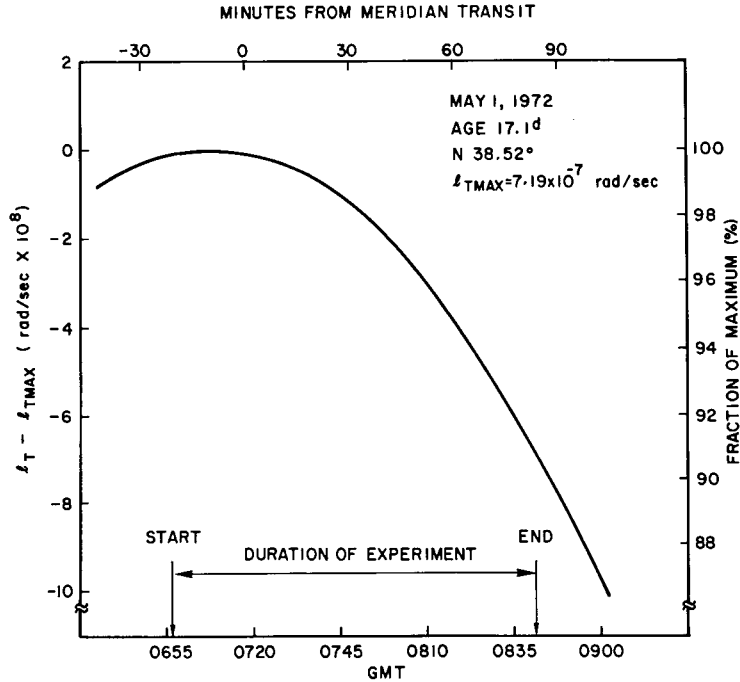


Fig. 2 — Total libration rate l_T for duration of experiment

Because of the low repetition rates and short pulse widths used in the experiment, the signal took up a small portion of the period corresponding to a single sweep. Moon echoes have a total range spread of 11.6 ms (in units of travel time), but the quasi-specular component of interest here is the dominant part of the return for the first couple of milliseconds at the operating RF frequency. Thus, the analog signal to be digitized was broken up into "digitizing windows" a few milliseconds long. During any given period of the incoming signal, the CDC 1604B computer directed sampling of the signal within the preset window, dumped the data during the off time of the window to digital magnetic tape units (MTU) at a rate comparable with the MTU's speed, and got ready for the next period. Hence records stored in the digital magnetic tapes belonged to different but consecutive periods of the lunar echoes. The digital datum $x(i, j)$ was then a function of the i th period (or record number) measured from the start of the digitizing run and the j th time sample measured from the start of the digitizing window. This kind of format synchronization allowed for continuous sampling of time histories at the desired time intervals.

STATISTICAL CHARACTERISTICS

Average Moon Echo

Figures 3-7 show the shape of the average Moon echo signal power from the time radar pulses impinge on the Moon (negative relay region) to a few hundred microseconds'

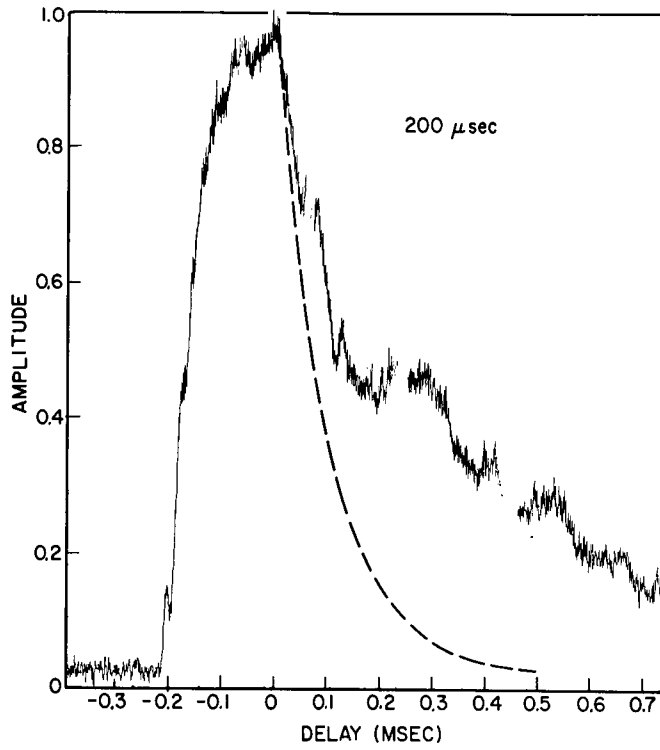


Fig. 3 — Average moon echo, 200-μs transmitted pulse width

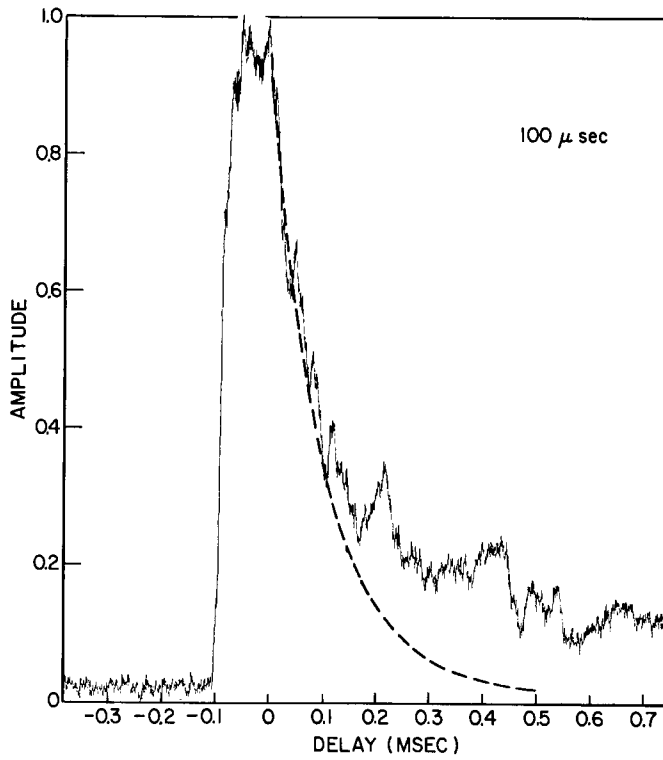


Fig. 4 — Average moon echo, 100-μs transmitted pulse width

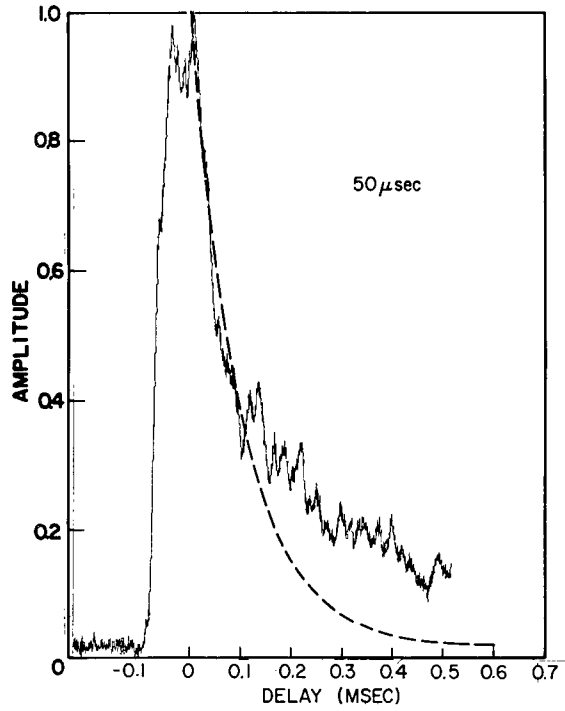


Fig. 5 — Average moon echo, 50- μ s transmitted pulse width

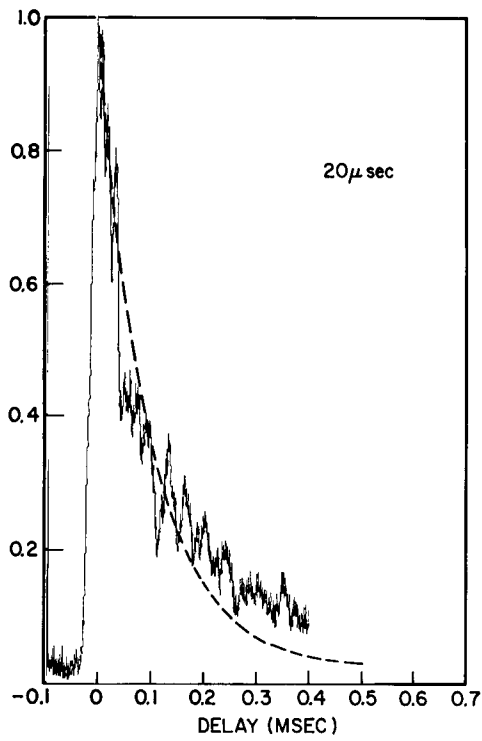


Fig. 6 — Average moon echo, 20- μ s transmitted pulse width

NRL REPORT 7717

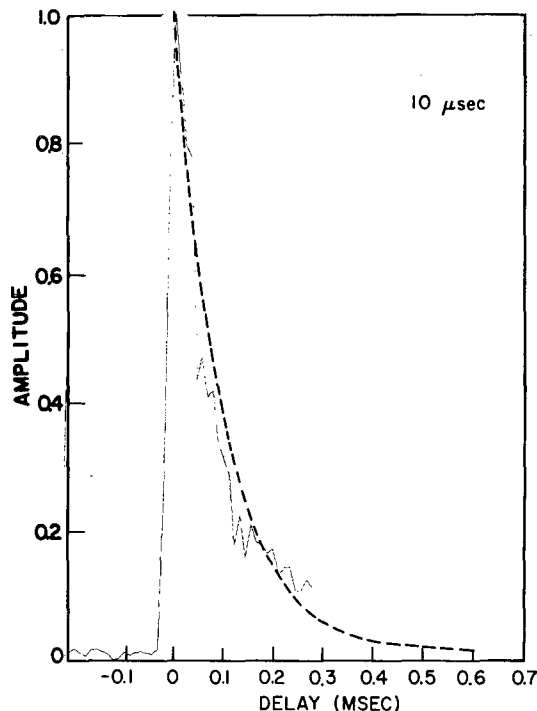


Fig. 7 — Average moon echo, 10- μ s transmitted pulse width

delay. These curves were obtained by computer programming a cumulative average of the digitized datum $x(i, j)$ in the form

$$\overline{x(j)} = \frac{1}{N} \sum_{i=1}^N x(i, j) \quad (2)$$

and plotting it vs $j\Delta t$, where N is the total number of echoes averaged in for each transmitted pulse-width sequence and Δt is the intersample interval 1/562.5 ms. The ratio of N over the PRF is the real time elapsed during digitizing for a particular pulse-width sequence. Table 1 summarizes the elapsed times for each sequence. The zero delay point was chosen to be the instant corresponding to maximum signal power. It is interesting to note in Figs. 3-7 that the shape of the scattered power in the positive delay region is basically the same for different transmitted pulse widths. The only exception might be the 200- μ s echo, Fig. 3. In fact, an exponential function of the form $\exp(-t/a)$ has been drawn in dashed lines on these figures and found to fit the delay tails rather well when $a = 100 \mu$ s. This behavior is consistent with previously obtained results for pulse widths of the order of 10 μ s at similar RF frequencies [2,9]. However, for pulse widths longer than 10 μ s, the total shape of the received-echo power (both positive and negative delays) is better fitted by a function of the form

$$f(t) = [U(t + T) - U(t)] + [\exp(-t/a)] U(t) \quad (3)$$

where t is delay time, T is the transmitted pulse width, a is a constant presumably dependent upon the RF frequency, and $U(t)$ is the unit step function. For example, the

the 100- μ s average Moon echo, Fig. 4, is reasonably fitted by

$$f(t) = [U(t + 100) - U(t)] + [\exp(-t/100)] U(t)$$

where t is measured in microseconds of delay. The rounding of the corners, most noticeable in Figs. 3 and 5, may be attributed in part to rough surface effects: scattered echoes from mountain peaks and sides arrive ahead of the time they would arrive had they been reflected from the mean surface, while those scattered from the flatlands arrive later. It might be possible to relate this spread of the leading edge of the lunar echo to a surface roughness coefficient, as has been done for space-radar altimeter returns in geodetic applications [11]. Such interpretation of the data, however, assumes a highly stable frequency source common to the radar system and the digitizing clock in order to minimize pulse-to-pulse jitter. Such a reference source was not provided in this experiment and hence the rounding of the corners may also be due in part to the data drifting across the digitizing window.

Table 1
Elapsed Time for Each Pulse Width Sequence

Pulse width (μ s)	PRF (Hz)	N (No. of Records)	Elapsed time (s)
200	25	1000	40
100	50	1000	20
50	100	4000	40
20	250	8000	32
10	500	8000	16

Autocorrelation Functions

Another characteristic of importance in the study of stochastic signals is the signal autocorrelation function, defined as

$$R(j, k) = \frac{\frac{1}{N} \sum_{i=1}^N \{ [x(i, j) - \bar{x}(j)] [x(i, k) - \bar{x}(k)] \}}{\bar{x}(j)\bar{x}(k)},$$

where

$$\bar{x}(j) = \frac{1}{N} \sum_{i=1}^N x(i, j)$$

$$\bar{x}(k) = \frac{1}{N} \sum_{i=1}^N x(i, k)$$

$$\bar{\bar{x}}(j) = \left\{ \frac{1}{N} \sum_{i=1}^N [x(i, j) - \bar{x}(j)]^2 \right\}^{1/2}$$

$$\bar{\bar{x}}(k) = \left\{ \frac{1}{N} \sum_{i=1}^N [x(i, k) - \bar{x}(k)]^2 \right\}^{1/2}.$$

Notice that Eq. (4) indicates a statistical averaging over the data sample space, as opposed to a time averaging over echo duration. Thus, it represents an ensemble autocorrelation and not a time autocorrelation. In weak stationarity conditions, such as those assumed here, the random processes are unaffected by translations of the origin for time. The autocorrelations $R(j, k)$ now depend only on the separation $\beta = k - j$ so that $R(j, k) = R(\beta)$. The resolving power of correlation function computation $\Delta\tau$ is then the total lag time divided by the number of lag steps. In our study of Moon echo data, the correlation matrix given by Eq. (4) was computed for the various pulse-width sequences and $R(\beta = k - 1)$ was plotted vs $\alpha = (k - 1)\Delta\tau$. The total lag time varied from sequence to sequence, depending upon record length and region of interest, but the total number of steps k was fixed at 178.

The Moon echo signals used in this study were, to some degree, corrupted by white noise. To better interpret trends in the autocorrelation function of the data, $R(\alpha)$ for noise time samples was computed and plotted in Fig. 8 for a 1.33- μ s resolution. If the bandpass of the white noise had been a boxcar function of width B Hz, $R(\alpha)$ would have had a $(\sin \alpha B)/\alpha B$ dependence. However, the diode detector used in the acquisition of the data probably had a tapered frequency response that enlarged the main lobe and reduced the side lobes of the expected $(\sin \alpha B)/\alpha B$ function; hence, the shape shown in Fig. 8, a very sharp spike centered about $\alpha = 0$ of 14 μ s width at the zero crossover and an essentially featureless character thereafter. Therefore, except for a difference in level at $\alpha = 0$, ensemble autocorrelation of the data for a large number of records yields the ensemble autocorrelation of the noiseless signal.

In Fig. 9 we show the ensemble autocorrelation of the 100- μ s scattered pulse for a 3.1- μ s resolution. As may be noticed, the function persists in a quasi-periodic mode even for long lags. This periodic component, although somewhat unexpected, has been observed previously in Moon echo studies [12-15] and has been attributed to the large-scale features of the lunar terrain. A curve fit to Fig. 9 for the first few hundred microseconds results in a correlation function of the form

$$R(\alpha) = A \frac{\sin\left(\frac{\pi\alpha}{T_1}\right)}{\left(\frac{\pi\alpha}{T_1}\right)} + B \cos\left(\frac{2\pi}{T_2}\alpha\right), \quad (5)$$

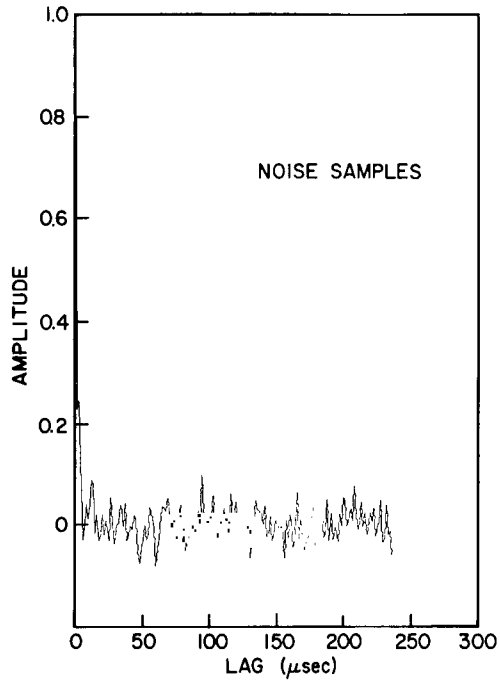


Fig. 8 — Autocorrelation function of noise time samples.

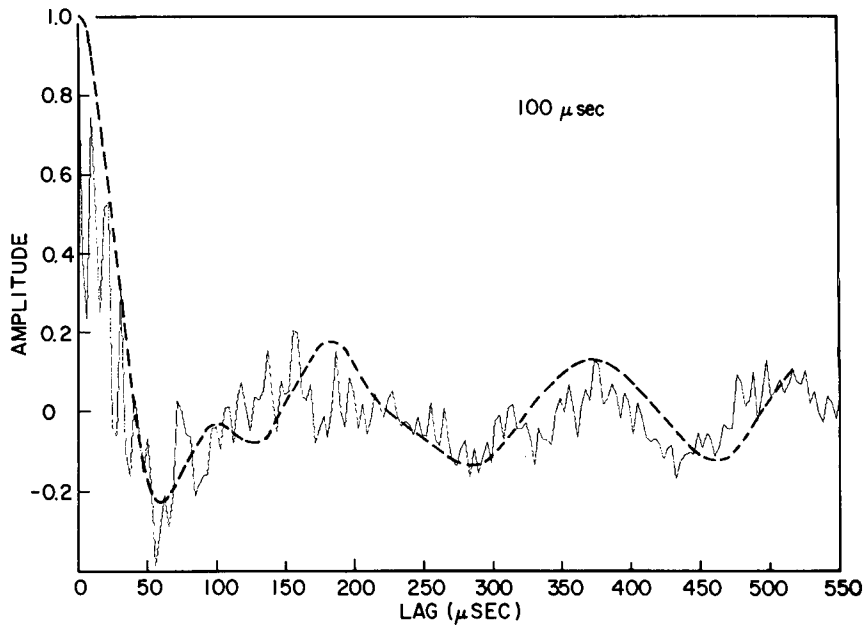


Fig. 9 — Moon echo autocorrelation function, 100- μs transmitted pulse width

where $T_1 = 42 \mu\text{s}$, $T_2 = 195 \mu\text{s}$, $A = 0.873$, $B = 0.127$, and α is lag time measured in microseconds. Examination of the autocorrelation plots of the 200-, 50-, and 20- μs scattered pulses, Figs. 10, 11 and 12 respectively, reveals a lag dependence similar to that given by Eq. (5). Table 2 summarizes the values of T_1 and T_2 for the various transmitted pulse widths and the corresponding correlation resolutions. We note that the T_1 parameter, which is one measure of the signal randomness, varies in rough proportion to the transmitted pulse width. However, the period of the quasi-periodic component T_2 is fairly independent of pulse width. This is indicative of the signal having a uniform power spectrum of width roughly proportional to the reciprocal of the pulse width, with a peaked spectral component, i.e., having the form of narrowband noise. No periodicity is detectable in the 20- μs correlation function, Fig. 12. This may be caused by a decrease in the signal-to-noise ratio of the data due to lunar echo modulation losses [2]. In this case, the noise variance for the total number of records averaged is such that it obscures the quasi-periodic component of the signal autocorrelation. In fact, no features were discernible in the autocorrelation plot for the 10- μs Moon echo on account of an even lower signal-to-noise ratio. Although a greater number of records N could have been correlated to decrease the noise variance, this was undesirable since the libration rate then would not be nearly uniform for the entire run, and nonstationary statistics might have been generated.

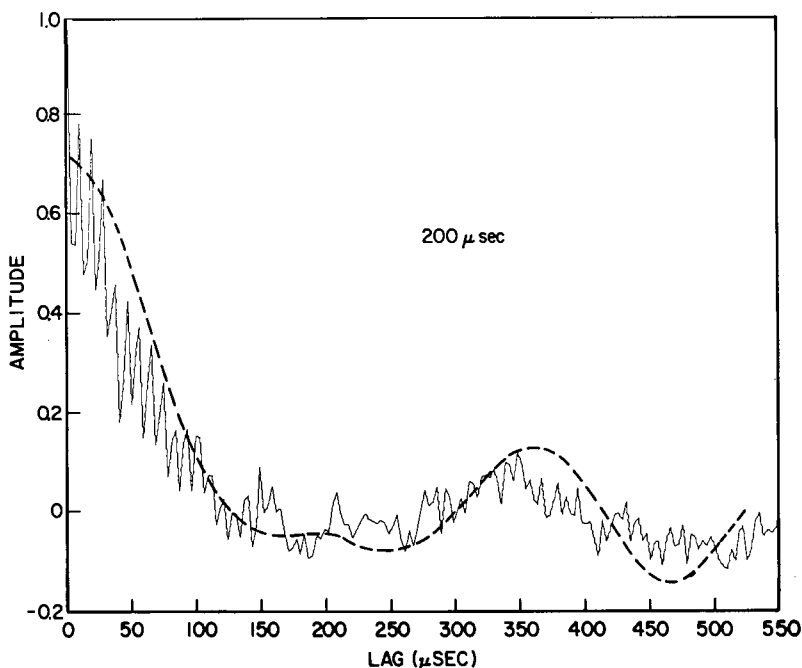


Fig. 10 — Moon echo autocorrelation function,
200- μs transmitted pulse width

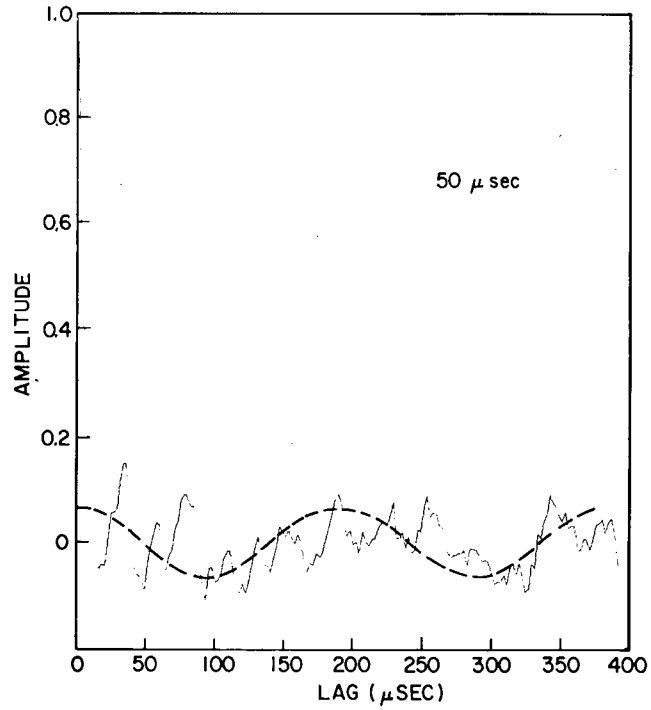


Fig. 11 — Moon echo autocorrelation function, 50- μ s transmitted pulse width

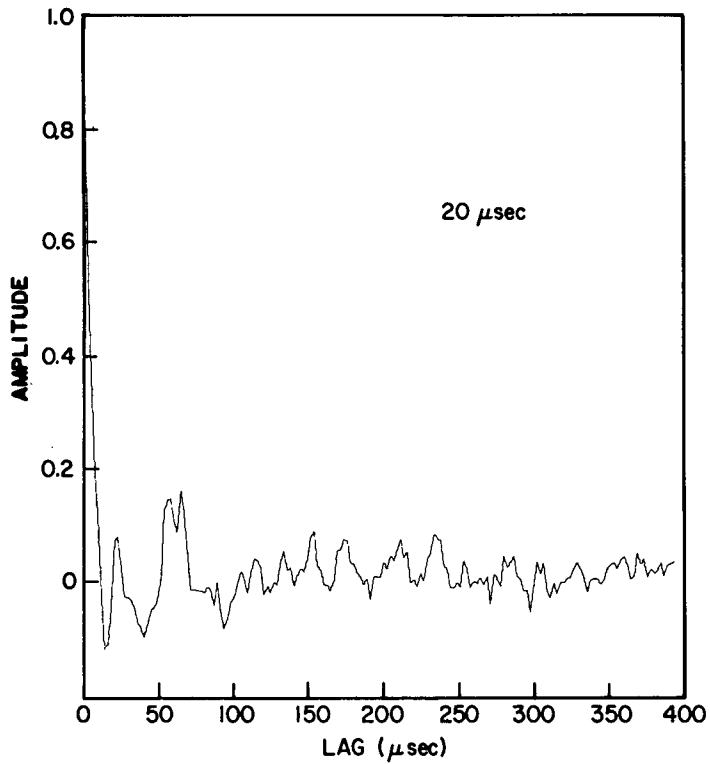


Fig. 12 — Moon echo autocorrelation function, 20- μ s transmitted pulse width

Table 2
Summary of Echo Autocorrelation Parameters for Each Pulse Width Sequence

Pulse width (μs)	T_1 (μs)	T_2 (μs)	Correlation Resolution (μs)
200	130	190	3.1
100	42	195	3.1
50	14	190	2.2
20	8.7	-	2.2

Sample Probability Density Functions

The theoretical distribution on Moon echo fluctuations at a fixed range $x(i, j = \text{constant})$ is a Rayleigh distribution [1]. This is actually the square root of a chi-square distribution with two degrees of freedom. The probability density function (PDF) of such a distribution is given as

$$g(x) = \left(\frac{x}{\sigma^2}\right) \exp\left(\frac{-x^2}{2\sigma^2}\right) \quad (6)$$

where

$$E[x^2] = \int_0^{\infty} x^2 g(x) dx = 2\sigma^2. \quad (7)$$

Previous observation of pulse fluctuations at an S-band frequency of 2860 MHz [16] have indicated that their distribution tended toward Rayleigh as the delay at which the amplitudes were sampled increased. To show that Moon echo amplitudes in the present investigation also appear to follow a Rayleigh distribution, Eq. (6) was fitted to sample histograms of echo amplitude fluctuations at a fixed delay of 50 μs for different transmitted pulse widths. Figures 13-16 show these histograms and the corresponding curve fits, with the axis of ordinates normalized to yield values for the sample PDF and the axis of abscissas normalized with respect to the sample standard deviation. The curve fits were performed following a recently suggested data display technique [17]. First an estimate $\hat{\sigma}^2$ of σ^2 was obtained by computing the variance of the data for a number of pulses and substituting it into Eq. (7). Then using this estimate $\hat{\sigma}^2$, the value of $g(x)$ at the center point x_j of each histogram interval was calculated from Eq. (6) and the difference between $g(x)$ and the sample PDF, the so-called residue $r(x_j)$, was formed. Figure 13b shows an example of the residues $r(x_j)$ plotted vs normalized pulse amplitude for the 200- μs transmitted pulse-width case. Figure 13c shows an inverted Rayleigh distribution for the same case. The total area under the residues was subsequently computed and the above procedure repeated for σ^2 slightly different from $\hat{\sigma}^2$. That value of σ^2 which minimized the total area under the residues was chosen as providing the best fit. This curve-fitting method had the effect of contrasting the data to yield a good display of the distribution of the pulse fluctuations about the assumed PDF. As can be seen in Figures 13-16 the solid lines are good fits to the apparently Rayleigh-distributed data.

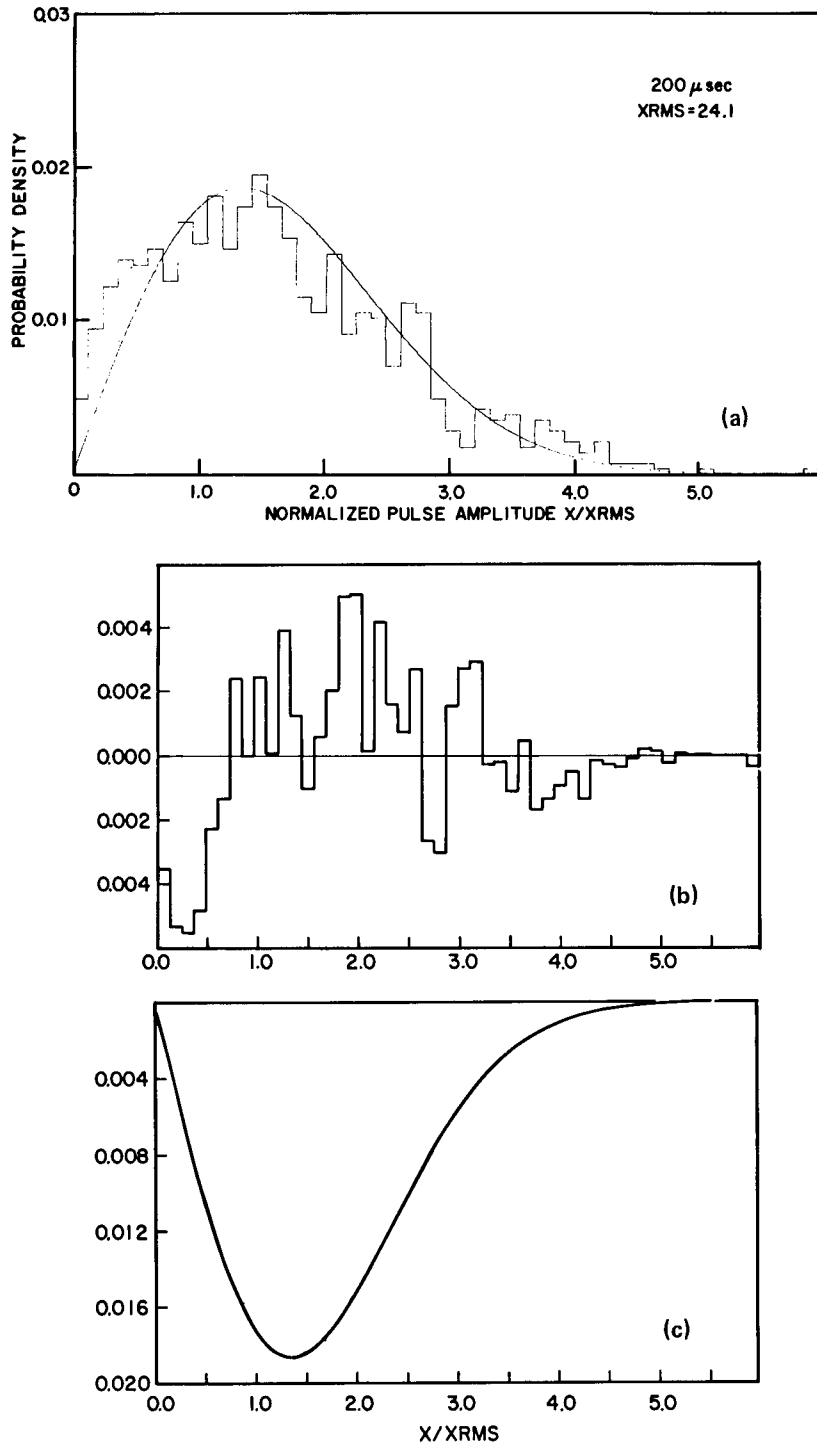


Fig. 13 — Moon echo (a) sample probability density function (b) residue plot (c) Rayleigh distribution, for a 200- μ s transmitted pulse width at a 50- μ s delay.

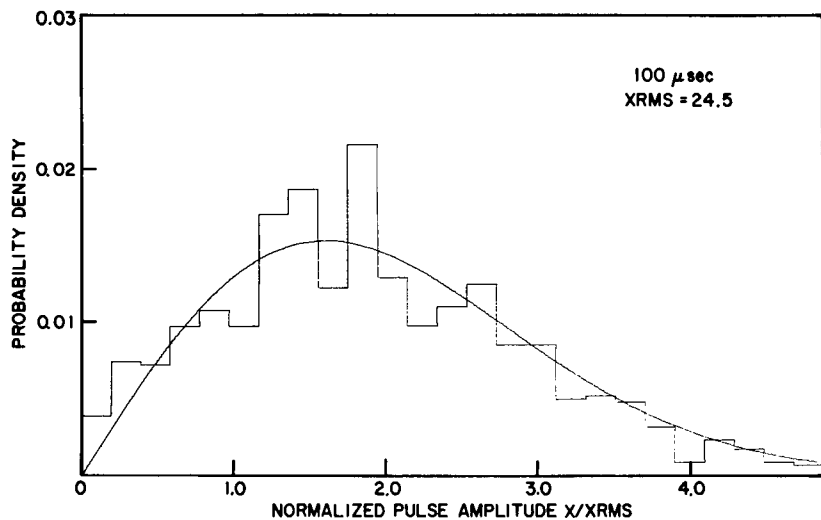


Fig. 14 — Moon echo sample probability density function for a 100- μ s transmitted pulse width at a 50- μ s delay

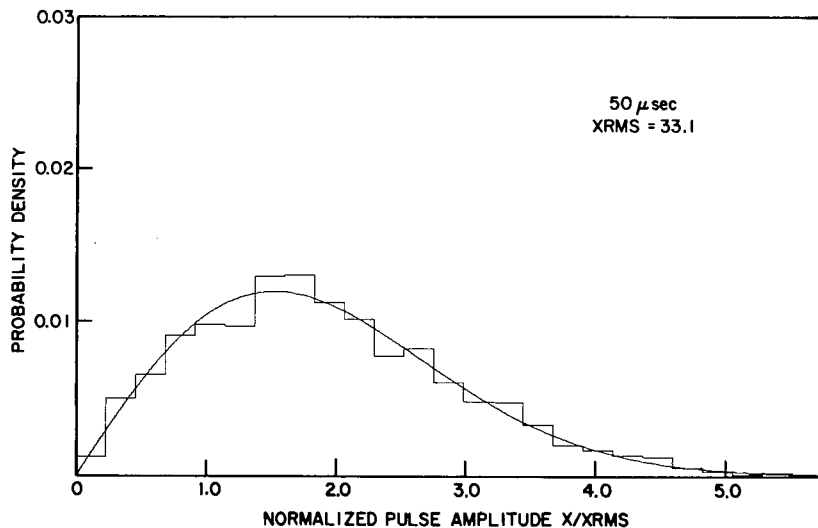


Fig. 15 — Moon echo sample probability density function for a 50- μ s transmitted pulse width at a 50- μ s delay

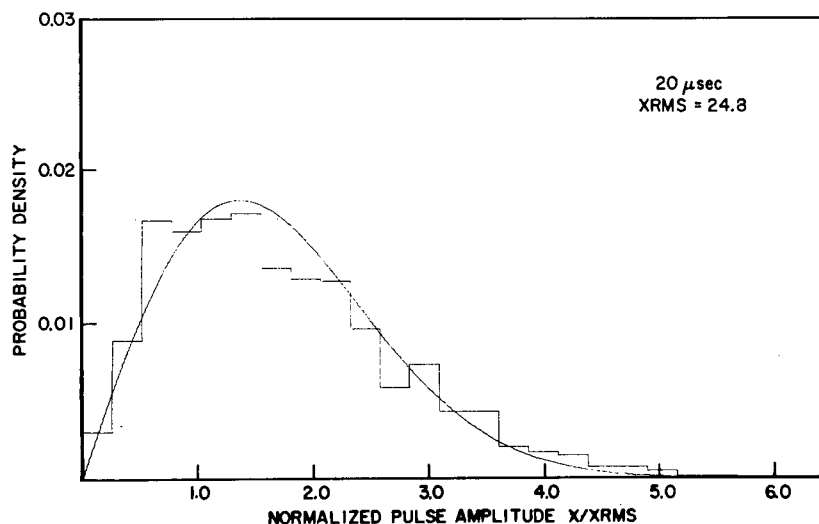


Fig. 16 — Moon echo sample probability density function for a 20- μ s transmitted pulse width at a 50- μ s delay

CONCLUDING REMARKS

In summary, this report presents an analysis of observations of the quasi-specular component of radar Moon echoes at a radio frequency of 138.6 MHz with pulse width as a parameter. The following conclusions have been drawn.

1. The form of the average waveform consists of two parts; the first one has a constant level of duration roughly equal to the transmitted pulse width, and the second one an exponential decay independent of pulse width.
2. The returns behave like random narrowband signals of bandwidth roughly proportional to the reciprocal of the transmitted pulse width, but with a peaked spectral component independent of transmitted pulse width.
3. The echo fluctuations about the exponential portion of the average waveform tend to have a Rayleigh probability density function independent of pulse width.

These conclusions should prove helpful in the design and evaluation of Moon echo signal-processing techniques using these statistical properties of the signal as their starting point.

ACKNOWLEDGMENT

The author acknowledges the valuable programming assistance of Mrs. B. Terry Caruthers, Code 7817TC, in the statistical computation routines.

REFERENCES

1. P. Beckmann and A. Spizzichino, *The Scattering of Electromagnetic Waves from Rough Surfaces*, Pergamon Press, New York, 1963.
2. J.H. Trexler, "Lunar Radio Echoes," *Proc. IRE* 46, 286-292 (Jan. 1958).
3. S.J. Fricker, R.P. Ingalls, et al., "Characteristics of Moon-Reflected UHF Signals," M.I.T. Lincoln Lab Technical Report 187, Dec. 1958, AD 204519.
4. T.B.A. Senior and K.M. Siegel, "A Theory of Radar Scattering by the Moon," *J. Res. NBS* 64D, 217-229, (May-June 1960).
5. J.V. Evans, S. Evans, and J.H. Thomson, "The Rapid Fading of Moon Echoes at 100 MC/S," in *Paris Symposium on Radio Astronomy* (edited by R.N. Bracewell), Stanford University Press, Stanford, Calif., 1959.
6. V.A. Hughes, "Radio Wave Scattering from the Lunar Surface," *Proc. Phys. Soc. London*, 78, 988-997 (Nov. 1961).
7. P. Beckmann, "Scattering by Composite Rough Surfaces," *Proc. IREE*, 53, 1012-1015, Aug. 1965.
8. O.I. Yakovlev, S.S. Matyugov, and K.M. Shvachkin, "Parameters of Scattered Radio-waves and the Nature of the Lunar Surface from 'Luna-14' Data," *Radio Engineering Elec. Phys.*, 15, 1145-1150 (1970).
9. J.V. Evans and T. Hagfors, eds., *Radar Astronomy*, McGraw Hill, New York, 1968.
10. "Radar Studies of the Moon," in *Advances in Astronomy and Astrophysics*, Vol. 8, (edited by Zdenek Kopal), Academic Press, New York, 1971, p. 29.
11. W.J. Pierson and E. Mehr, "Average Return Pulse Form and Bias for the S193 Radar Altimeter on Skylab as a Function on Wave Conditions," in *The Use of Artificial Satellites for Geodesy* (edited by S.W. Henniksen), Geophysical Monograph 15, American Geophysical Union, Washington, D.C., 1972.
12. T.B.A. Senior and K.M. Siegel, "Radar Reflection Characteristics of the Moon," in *Paris Symposium on Radio Astronomy* (edited by R.N. Bracewell), Stanford University Press, Stanford, Calif., 1959.
13. V.A. Hughes, "Diffraction Theory Applied to Radio Wave Scattering from the Lunar Surface," *Proc. Phys. Soc. London*, 80, 1117-1127, 1962.
14. F.B. Daniels, "Radar Reflection from a Rough Moon Described by a Composite Correlation Function," *J. Geophys. Res.* 68, 6251-6254 (1963).
15. "Radar Reflection from a Planetary Surface Described by a Composite Correlation Function," TR-2314, Army Electronics Res. Dev. Center, Fort Monmouth, N.J. AD 408198, May 1963.

16. B.S. Yaplee, N.G. Roman, et al., "A Lunar Radar Study at 10 Cm Wavelength," in *Paris Symposium on Radio Astronomy* (edited by R.N. Bracewell), Stanford University Press, Stanford, Calif., 1959.
17. J.W. Tukey, "Exploratory Data Analysis," paper presented at American Association for the Advancement of Science Annual Meeting, Washington, D.C., Dec. 1972.